

Electronic Supplementary Information (ESI)
**Growth of hematite nanowire arrays during dense
pentlandite oxidation**

Huihui Zhu^a, Jinxia Deng^b, Jun Chen^a, Ranbo Yu^a, and Xianran Xing^{*a}

*a Department of Physical Chemistry, University of Science & Technology Beijing, Beijing
100083, PR China*

*b Department of Chemistry, University of Science & Technology Beijing, Beijing 100083, PR
China*

**Corresponding Author: Tel: +86 10 62334200; fax: +86 10 62332525 E-mail address:
xing@ustb.edu.cn*

Synthesis of pentlandite

Pentlandite (Fe,Ni)₉S₈ was prepared through the traditional dry silica-tube route using purity elemental Fe, Ni, and S as starting materials. Accurately weighed stoichiometric amounts of Fe, Ni and S (Fe_{4.5}Ni_{4.5}S₈) were sealed under vacuum in 10mm diameter silica tubes. The charge was heated slowly (1°C/min) to 500°C, with subsequent heating to 700°C, soaking for 3h at each stage. This slow heating and soaking program were employed to avoid tube breakage resulted from the high sulfur vapor pressure above 450°C. Following that, the charge was heated to 1150°C and soaking for 12h, and then allowed to cool to room temperature slowly. The charge was removed from the tube and ground into fine powder with acetone, ensuring the homogeneity of the pentlandite. The charge was then resealed in silica tube and heated at 1150°C for 10h, and then cooled to room temperature slowly. Finally, homogenous pure pentlandite with a thin pyrrhotite coating on the products was obtained.

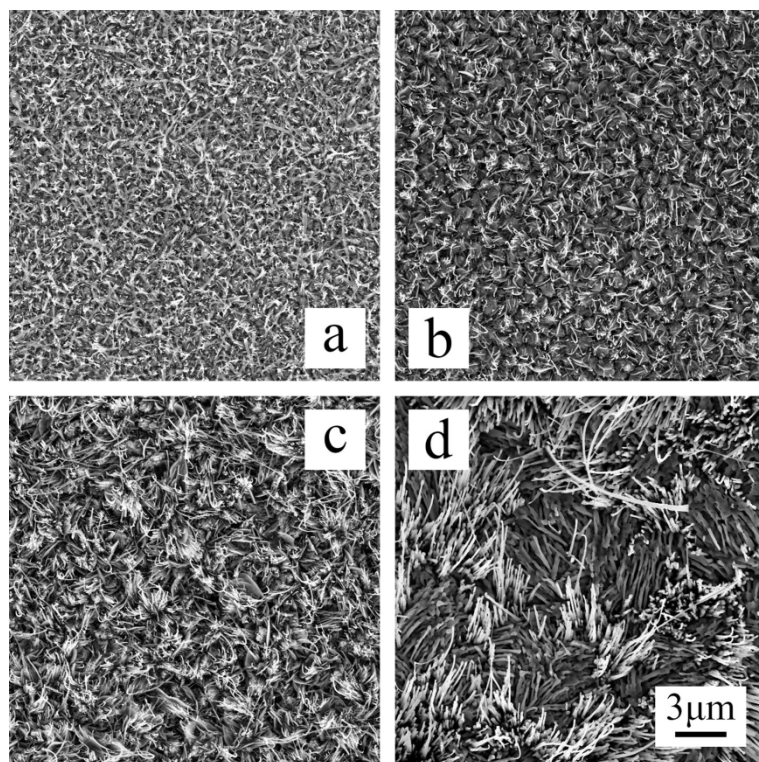


Fig S1. SEM images taken after 10 min oxidation for dense pentlandite. (b) 30 min. (c) 2 h. (d) 24 h.

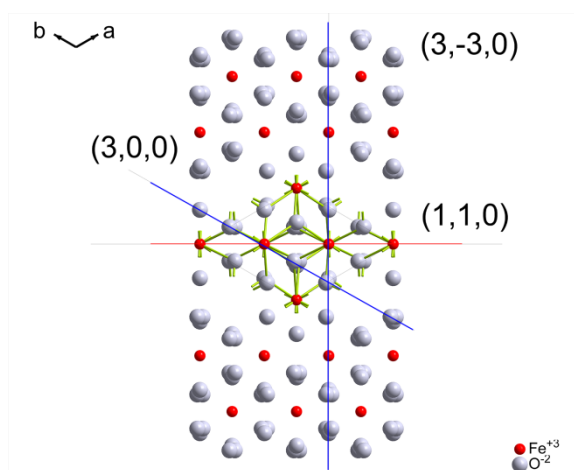


Fig. S2 Atomic model of hematite, assigned the locations of (110), (300) and $(3\bar{3}0)$ planes.

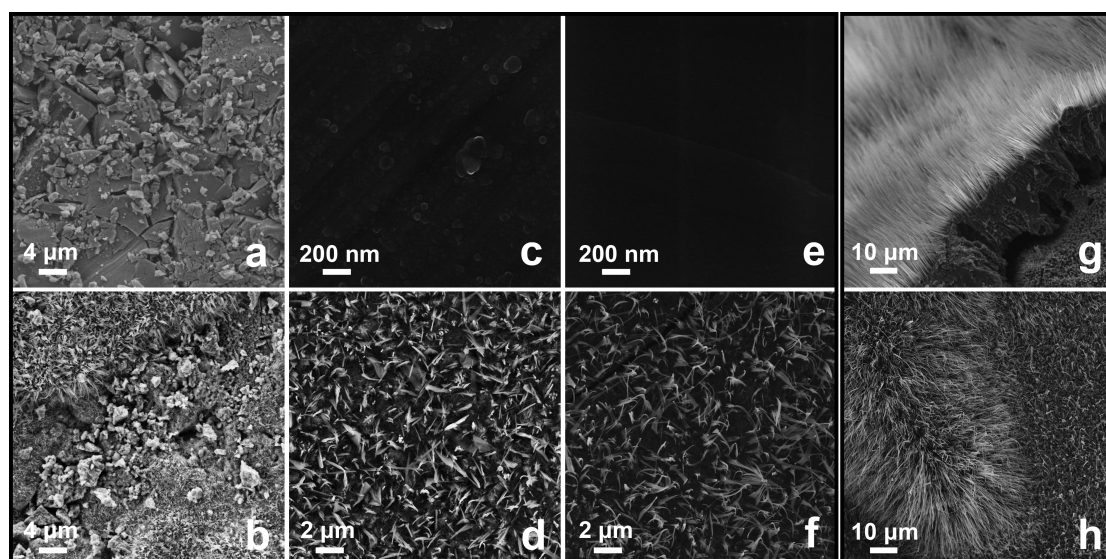
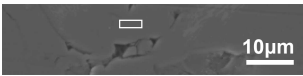
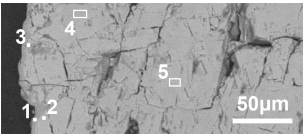
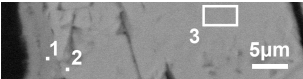
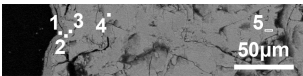
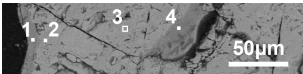
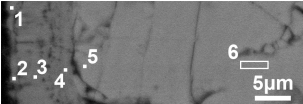
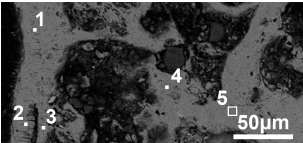
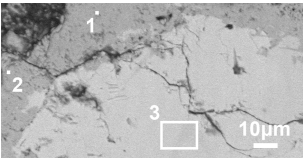
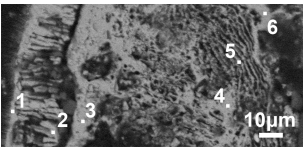


Fig. S3 SEM images of (a) pentlandite piece compressed from powder before oxidation, (b) sample like (a) oxidized 10 min, (c) dense pentlandite piece sliced and polished before oxidation, (d) sample like (c) oxidized 10 min, (e) broken surface of dense pentlandite piece (without slicing or polishing), (f) sample like (e) oxidized 10 min, (g) sample like (c) oxidized 24 h, (h) sample like (e) oxidized 24 h.

Fig. S3 shows the comparison of different pentlandite substrates. There were not uniform $\alpha\text{-Fe}_2\text{O}_3$ nanostructures on the pentlandite piece which was compressed from powder for 10 min oxidation. (Fig. S3 a b) Some have grown very long, some just a little. On the surfaces of dense pentlandite, both sliced piece and broken piece, there were uniform $\alpha\text{-Fe}_2\text{O}_3$ nanostructures after 10 min oxidation, but those on broken piece were more scattered. (Fig. S3 d f) A few oxidized particles could be found on the surface of sliced and polished sample. (Fig. S3 c) However, the surface of broken sample was very smooth except fracture line. (Fig. S3 e) Although they have been exposed in air for the same time. After 24 h oxidization, dense and uniform $\alpha\text{-Fe}_2\text{O}_3$ nanowire arrays grew from surface of sliced and polished sample. But of broken sample, nanostructures were dense and long on some areas, scattered and short on other areas. The results implied that the nucleation and growth of $\alpha\text{-Fe}_2\text{O}_3$ nanowires could be effected by both the surface texture (grain orientation) of dense pentlandite and surface treatment process.

Table S1. EDX composition analysis data.

Sample	SEM Image	No.	Atom %				M/S	Fe/Ni (sulfide)	M/O	
			O	S	Fe	Ni				
Pn		1	-	48.72	25.98	25.30	1.05	1.03	-	
10 min		1	55.92	0.25	43.83	-	-	-	0.78	
		2	-	48.66	19.69	31.64	1.05	0.62	-	
		3	-	48.35	16.06	35.59	1.07	0.45	-	
		4	-	52.71	27.51	19.78	0.90	1.39	-	
		5	-	49.41	22.80	27.79	1.02	0.82	-	
		1	52.59	-	46.81	0.60	-	-	0.90	
		2	-	48.51	17.88	33.61	1.06	0.53	-	
		3	-	49.49	22.43	28.07	1.02	0.80	-	
	30 min		1	52.51	-	47.49	-	-	-	0.90
			2	41.56	12.81	37.57	8.07	-	-	-
3			-	48.67	20.05	31.27	1.05	0.64	-	
4			-	48.95	21.73	29.32	1.04	0.74	-	
5			-	48.95	22.79	28.26	1.04	0.81	-	
2 hours		1	49.89	-	50.11	-	-	-	1.00	
		2	-	53.13	26.92	19.96	0.88	1.35	-	
		3	-	49.12	23.69	27.19	1.04	0.87	-	
		4	21.04	7.81	62.01	9.14	-	-	-	
		1	61.22	0.29	38.48	-	-	-	0.63	
		2	53.19	-	46.81	-	-	-	0.88	
		3	53.28	-	46.72	-	-	-	0.88	
		4	48.60	0.50	50.15	0.75	-	-	-	
		5	-	48.78	20.41	30.81	1.05	0.66	-	
		6	-	48.67	18.26	33.07	1.05	0.55	-	
24hours		1	54.00	-	46.00	-	-	-	0.85	
		2	44.34	-	55.66	-	-	-	1.26	
		3	51.16	-	48.06	0.78	-	-	0.95	
		4	49.68	-	45.21	5.10	-	-	1.01	
		5	50.73	-	46.13	3.14	-	-	0.97	
		1	49.79	-	47.54	2.67	-	-	1.01	
		2	51.57	-	42.47	5.96	-	-	0.94	
		3	-	49.72	1.07	49.21	1.01	0.02	-	
		1	59.19	-	40.81	-	-	-	0.69	
		2	57.70	-	42.30	-	-	-	0.73	
		3	49.86	-	49.72	0.42	-	-	1.01	
		4	51.68	-	45.47	2.86	-	-	0.94	
		5	47.93	-	46.99	5.08	-	-	1.09	
		6	41.90	-	51.39	6.71	-	-	1.39	

1. V. A. Drebuschak, T. A. Kravchenko and V. S. Pavlyuchenko, *J. Cryst. Growth*, 1998, **193**, 728-731.
2. F. Xia, J. Zhou, J. Brugger, Y. Ngothai, B. O'Neill, G. Chen and A. Pring, *Chem. Mater.*, 2008, **20**, 2809-2817.
3. H. Zhu, J. Chen, J. Deng, R. Yu and X. Xing, *Metall. Mater. Trans. B*, 2012, **43**, 494-502.